



AUSTRALIAN ATOMIC ENERGY COMMISSION
RESEARCH ESTABLISHMENT
LUCAS HEIGHTS

NEUTRON ENERGY SPECTRA FROM THE THICK TARGET
 ${}^9\text{Be}(d,n){}^{10}\text{B}$ REACTION

by

S. WHITTLESTONE

December 1976

ISBN 0 642 99764 0

AUSTRALIAN ATOMIC ENERGY COMMISSION
RESEARCH ESTABLISHMENT
LUCAS HEIGHTS

NEUTRON ENERGY SPECTRA FROM THE THICK TARGET
 ${}^9\text{Be}(d,n){}^{10}\text{B}$ REACTION

by

S. WHITTLESTONE

ABSTRACT

The energy spectrum of neutrons emitted when deuterons impinge on a thick beryllium target has been measured using an NE213 scintillation detector and the time-of-flight technique. Spectra were measured at angles of 0, 30, 45, 60, 90, 120 and 150° for deuteron energies of 1.4, 1.8, 2.3 and 2.8 MeV. Tables are presented of these angle-dependent energy spectra, the angle-integrated energy dependent yields, and the total neutron yield as a function of deuteron energy.

National Library of Australia card number and ISBN 0 642 99764 0

The following descriptors have been selected from the INIS Thesaurus to describe the subject content of this report for information retrieval purposes. For further details please refer to IAEA-INIS-12 (INIS: Manual for Indexing) and IAEA-INIS-13 (INIS: Thesaurus) published in Vienna by the International Atomic Energy Agency.

ANGULAR DISTRIBUTION; BERYLLIUM 9 TARGET; BORON 10; DEUTERON REACTIONS; ERRORS; MeV RANGE 01-10; NEUTRON SPECTRA; NEUTRONS; NUCLEAR REACTION YIELD; TIME-OF-FLIGHT METHOD

CONTENTS

	<u>Page</u>
1. INTRODUCTION	1
2. EXPERIMENTAL METHOD	1
2.1 Time-of-Flight Measurement Facility	1
2.2 Background Determination	2
2.3 Data Analysis	3
2.4 Errors	4
3. RESULTS	4
4. CONCLUSIONS	5
5. ACKNOWLEDGEMENTS	5
6. REFERENCES	5
Tables 1-4	Angle-dependent neutron energy spectra from the thick target ${}^9\text{Be}(d,n){}^{10}\text{B}$ reaction, with bombarding deuteron energies of 1.4, 1.8, 2.3 and 2.8 MeV.
Table 5	Calculated maximum neutron energies (MeV) from the ${}^9\text{Be}(d,n){}^{10}\text{B}$ reaction
Table 6	Angular distributions from the thick target ${}^9\text{Be}(d,n){}^{10}\text{B}$ reaction for neutrons with energies above three energy thresholds
Table 7	Total neutron yield above different threshold energies
Figure 1	Pulse height spectra from scintillator
Figure 2	Angle-dependent neutron energy spectra from the ${}^9\text{Be}(d,n){}^{10}\text{B}$ reaction for deuteron energy 1.4 MeV
Figure 3	Angle-dependent neutron energy spectra from the ${}^9\text{Be}(d,n){}^{10}\text{B}$ reaction for deuteron energy 2.8 MeV
Figure 4	Angle-integrated neutron energy spectra
Figure 5	Angular distributions from the thick target ${}^9\text{Be}(d,n){}^{10}\text{B}$ reaction for neutrons with energies greater than 0.25 MeV.

1. INTRODUCTION

Some neutronics experiments [Moo et al. 1973] and neutron radiotherapy [Cotterall et al. 1971] require an intense ($\sim 5 \times 10^{11}$ neutrons s^{-1}) source of neutrons. When this source is based on a particle accelerator limited to 3 MV or less, the most prolific neutron sources available are beryllium and lithium bombarded by deuterons. Beryllium is superior to lithium in several respects; for example, its mechanical, chemical and heat conductivity properties permit target construction which withstands prolonged exposure to beams of the order of 200 μA . Also, the neutron energy spectrum from the ${}^9\text{Be}(d,n){}^{10}\text{B}$ reaction ranges from zero to a few MeV, making this reaction more suitable for some applications than the ${}^7\text{Li}(d,n){}^9\text{Be}$ reaction which produces neutrons with energies up to 14 MeV.

Many potential uses of beryllium as a neutron source require that the energy spectrum be well known. The only comprehensive measurement of the ${}^9\text{Be}(d,n){}^{10}\text{B}$ reaction in the deuteron energy range 1 to 3 MeV has been made by Inada et al. [1968]. A spectrum measurement made at this laboratory disagreed with that of Inada et al. and motivated the present series of measurements. Although the present measurements use a pulsed time-of-flight technique similar to that of Inada et al., the energy resolution has been improved by using a longer flight path and more advanced analysis. Moreover, the number of neutrons scattered from the floor into the detector have been reduced by using an elevated target facility. Difficulties of interpretation introduced by collimators or shields were thereby avoided.

Only the detailed experimental method and results are presented here. Technical aspects of the time-of-flight facility and comparison of the results with those of Inada et al. will be given in separate publications [Whittlestone 1977a, 1977b].

2. EXPERIMENTAL METHOD

2.1 Time-of-Flight Measurement Facility

A pulsed deuteron beam from a 3 MV Van de Graaff accelerator was transported by means of two bending magnets to a 3 mm thick, air-cooled beryllium target 5 m above the floor and 6 m from the nearest concrete shield wall. The neutron detector, a 50 mm diameter by 36 mm NE213 scintillator, was mounted 2.26 m from the target. Its lower threshold was set to 0.224 times the mean amplitude of the photopeak from the 0.0596 MeV γ -ray emitted by ${}^{241}\text{Am}$. At this setting the neutron energy threshold was about 200 keV.

2.2 Background Determination

The background could be divided into two parts, the neutrons or γ -rays which were scattered from nearby objects, and those which came directly from the target but which were generated by the residual deuteron beam present when the pulsing system had swept the central core of the beam away from the chopping aperture. The first component was negligible [Whittlestone 1977a], but determination of the second component was complicated by the time dependence of the residual beam.

The background at the low energy end of the spectra was determined by using the scintillator as a proton recoil spectrometer, gated to measure pulse height spectra from different time windows after the beam pulse. The spectrum at any window was the sum of the spectra from two groups of particles: these were neutrons generated during the beam pulse, which will be referred to as 'primary' neutrons, and a combination of neutrons and γ -rays generated by the residual beam. The pulse height spectrum from this last component was the same as the spectrum from the target bombarded by a steady beam, and contained pulses much larger than the pulses from the low energy primary neutrons. It was therefore possible to determine the proportion of primary neutrons in any time window by matching the high pulse height part of the spectrum measured using the time window with the spectrum obtained from a steady beam. The excess counts at the low pulse height end of the window spectrum could be attributed to primary neutrons with energies corresponding to the time range covered by the window.

A typical pulse height spectrum, obtained with a time window set to include primary neutrons with energies between 0.077 and 0.178 MeV, is shown in Figure 1. The deuteron energy (E_d) was 2.4 MeV and the angle 0° . Also shown is a pulse height spectrum obtained with no time gating, scaled to match the gated spectrum at the normalisation point indicated. By subtracting the background from the gated spectrum, it was established that 62 per cent of the count was from primary neutrons. A window corresponding to a lower energy, between 0.040 and 0.077 MeV, yielded 26 per cent primary neutrons.

An examination of the time spectrum at $E_d = 2.4$ MeV and 0° showed that these proportions of primary neutrons could be reproduced by assuming a time-independent background equal to half the count in the channel at 0.073 MeV. Similar measurements and comparisons at 0° showed the same 'recipe' to be valid for the other three deuteron energies used, *i.e.* 1.4, 1.8 and 2.8 MeV. Since it was not feasible to measure time-dependent pulse

height spectra for all four deuteron energies (E_d) and seven angles and repeat them, the above recipe was used to calculate the background counts which should be subtracted from the low energy part of all the time-of-flight spectra. The major uncertainty in the recipe is the assumption that the pulse characteristics of the Van de Graaff accelerator did not change from one run to the next. Examination of the time-of-flight spectra indicated that variations of the order 50 per cent in background were possible. This would give rise to an error of about 4 per cent at 0.2 MeV, and about 25 per cent at 0.1 MeV in the energy spectra.

Background correction at the short flight time or high energy end of the spectrum was simpler because the background contribution was small. For example, with a deuteron energy of 2.8 MeV at 0° , the count in three channels above the high energy edge ($E_{\max} = 7.15$ MeV) was only about 2 per cent of the count in the peak at 6 MeV. The recipe obtained for estimating the background at long flight times was therefore applied to the whole spectrum, ignoring any time dependence. Although this simple approach underestimated the unwanted counts at the high energy end of the spectrum, the error introduced was insignificant. All spectra show a clearly defined edge at high energy corresponding to the ${}^9\text{Be}(d,n){}^{10}\text{B}$ reaction, leaving ${}^{10}\text{B}$ in its ground state. The few counts observed above this edge were the result of errors in the background determination and have been set to zero.

2.3 Data Analysis

After subtracting the background, the time-of-flight data were unfolded with respect to the time profile of the beam pulse, which was assumed to be the same as that of the gamma flash. An iterative conjugate gradient technique developed by Lang [1977] was used. The code essentially answers the question, 'What would the time spectrum be if the beam pulse profile were confined to one channel?' It is known that, given this ideal time spectrum, say $S(t)$, one can generate the time spectrum $T(t)$ obtained when the beam pulse profile is $R(t)$:

$$T(t) = \int_0^{\infty} R(t-t')S(t')dt' \quad \dots(1)$$

Given the observed time spectrum $T(t)$ and $R(t)$ (which in this case is the gamma flash spectrum), the code guesses a spectrum $S^1(t)$, then generates a $T^1(t)$ which it compares with the experimental $T(t)$. The difference is used to generate a second $S^2(t)$ and $T^2(t)$ and so on, until

$T^n(t)$ agrees with $T(t)$ within the statistical errors. $S^n(t)$ is then taken to be the desired unfolded time-of-flight spectrum of the neutrons.

Using this code, the effective time resolution was improved from the 5 ns full width at half maximum of the gamma flash to the 1.5 ns channel width used for measuring the time spectra. Since the flight path was just over 2 m, the energy resolution of the present work was a factor of four better than the resolution of the experiment by Inada *et al.* [1968]. The energy spectrum was obtained from the unfolded time spectrum in the usual way and, as a final step, the data at low energies were averaged over 50 keV intervals. No significant features of the spectra were lost by this procedure, but the quantity of the data to be tabulated was reduced substantially.

2.4 Errors

The four major sources of error were statistical fluctuations in the time spectra, uncertainties in the detector efficiency, background subtraction and normalisation of the individual spectra to units of neutrons per microcoulomb. In the tabulated data, the errors in the angle-dependent spectra include only the statistical error and the error in the efficiency of the detector. Uncertainties in the background have already been discussed. The additional error introduced by normalisation was 3 per cent. Details of how estimates for the errors in efficiency and normalisation were derived will be given elsewhere [Whittlestone 1977a].

Over most of the energy range, the errors on the individual angle-dependent energy spectra were about 5 per cent. Normalisation to neutron flux per microcoulomb increased the error to about 6 per cent. At low energies the errors were 7 per cent at 0.2 MeV increasing to about 35 per cent at 0.1 MeV.

3. RESULTS

The angle-dependent energy spectra are fully presented in Table 1-4 for deuteron energies 1.4, 1.8, 2.3 and 2.8 MeV, and angles 0, 30, 45, 60, 90, 120 and 150°. To simplify comparison with the results of Inada *et al.* [1968], these data have been expressed as neutron fluences at the detector for a target-detector separation of 1 m, and quoted in units of neutrons $\text{MeV}^{-1} \text{cm}^{-2} \mu\text{C}^{-1}$. Spectra at 0, 30, 60 and 150° for deuteron energies 1.4 and 2.8 MeV have been plotted in Figures 2 and 3.

The last two columns in Tables 1-4 give the value and error of the yield ($\text{MeV}^{-1} \mu\text{C}^{-1}$) formed by integrating the flux over a sphere. This result is also plotted in Figure 4.

For completeness, the maximum neutron energy expected at each angle and deuteron energy has been calculated using the Q value for the ground state transition as quoted by Lauritsen & Ajzenberg-Selove [1966]. These energies are given in Table 5.

Table 6 gives the angular distributions of neutron fluences for the Be(d,n) reaction, formed by integrating the angle-dependent energy spectra over energy above energy thresholds of 0.075, 0.25 and 0.95 MeV. The angular distribution with neutron energy threshold 0.25 MeV has been plotted in Figure 5. Finally, the angular distributions have been integrated to give the total neutron yield above the same three neutron energy thresholds. These yields are given in Table 7, which also gives the total yield for neutrons of all energies, estimated by extrapolating plots of the Table 6 data to zero neutron energy.

4. CONCLUSIONS

A comprehensive measurement of the angle-dependent neutron energy spectra from the ${}^9\text{Be}(d,n){}^{10}\text{B}$ reaction has been made for deuteron energies between 1.4 and 2.8 MeV. The spectra are accurate to about 6 per cent above a neutron energy of 0.2 MeV, and have an energy resolution limited by the channel width, which is 0.3 MeV at a neutron energy of 7 MeV.

Although the experiment was set up to measure spectra of neutrons with energies greater than 0.2 MeV, it was established that there is a significant number of neutrons at 0.1 MeV. There is, therefore, a need for a measurement of the neutron energy spectra in the range 0 to 0.2 MeV.

5. ACKNOWLEDGEMENTS

The author is grateful for discussions with Dr. A.I.M. Ritchie. The assistance of the technical staff associated with the Van de Graaff accelerator has also been most valuable.

6. REFERENCES

- Cotterall, M., Rogers, C.C., Thomlinson, R.H. & Fields, S.B. [1968] - Brit. J. Radiol., 44:603.
- Inada, T., Kawachi, K. & Hiramoto, T. [1968] - J. Nucl. Sci. Tech., 5:22.
- Lang, D. [1977] - AAEC/E398 (in press).
- Lauritsen, T. & Ajzenberg-Selove, F. [1966] - Nucl. Phys., 78:111.
- Moo, S.P., Rainbow, M.T. & Ritchie, A.I.M. [1973] - J. Nucl. En., 27:753.
- Whittlestone, S. [1977a] - AAEC/E report (in preparation).
- Whittlestone, S. [1977b] - J. Phys. D - submitted for publication.

TABLES 1-4

ANGLE-DEPENDENT NEUTRON ENERGY SPECTRA FROM THE THICK TARGET

${}^9\text{Be}(d,n){}^{10}\text{B}$ REACTION, WITH BOMBARDING DEUTERON ENERGIES

OF 1.4, 1.8, 2.3 AND 2.8 MeV.

TABLE 2

DEUTERON ENERGY 1.8 MeV

DEUTERON ENERGY ANGLE NEUTRON ENERGY	1.80		30	45	60	90	120	150	INTEGRATED 0-180							
	COUNT	ERROR							COUNT	ERROR	COUNT	ERROR	COUNT	ERROR		
C.100	25574	5785	17965	4011	18193	4303	19191	4455	18345	5398	23676	7365	22137	5435	2.553E+05	6.9E+08
O.150	8919	1504	5932	1003	6139	1079	6701	1154	6379	1274	9629	1894	8453	1430	9.362E+0E	1.7E+08
O.200	7348	653	4663	419	4556	442	4932	463	4803	558	7730	863	6568	594	7.224E+08	7.5E+07
O.250	7558	461	4465	280	4154	287	4435	295	4447	371	7279	582	6271	354	6.753E+08	5.0E+07
O.300	7731	426	4377	248	3957	243	4238	252	4314	310	6776	476	5663	326	6.386E+08	4.1E+07
O.350	7133	468	4172	227	3692	215	3900	222	3997	266	6313	410	5173	286	5.943E+08	3.6E+07
O.400	7526	393	3687	208	3320	188	3525	196	3669	232	5764	358	4311	236	5.853E+08	3.2E+07
O.450	7293	373	3655	191	3047	168	3218	174	3325	202	4788	291	2422	140	4.489E+08	2.6E+07
O.500	7643	373	3594	180	2946	155	3059	159	3138	182	3293	204	2123	117	3.907E+0E	2.2E+07
O.550	8116	397	3659	183	2885	151	2987	155	3056	174	2239	149	1945	108	3.553E+08	2.0E+07
O.600	8372	416	3678	195	2812	148	2819	147	2534	147	2125	140	1906	105	3.298E+0E	1.9E+07
O.650	8688	429	3610	182	2676	141	2657	139	1314	89	2012	131	1720	94	2.783E+08	1.6E+07
O.700	8651	479	3816	193	2801	147	2683	140	1360	87	1996	128	774	51	2.683E+08	1.5E+07
O.750	10381	536	4014	210	2776	150	2352	128	1272	84	1935	123	655	44	2.576E+08	1.5E+07
O.800	11133	580	3562	209	2421	133	1406	81	1297	84	747	67	570	39	1.990E+08	1.2E+07
O.850	11165	575	3799	198	1640	61	1279	70	1309	82	677	57	522	35	1.825E+0E	1.1E+07
O.900	11705	602	3119	163	1008	60	1196	68	1368	82	650	54	594	38	1.707E+0E	1.0E+07
O.950	11099	567	1119	64	985	57	1219	68	595	46	629	52	607	38	1.224E+0E	7.8E+06
1.000	3024	167	764	45	946	55	1140	65	409	35	741	56	611	38	9.623E+0E	6.4E+06
1.050	787	55	808	46	946	55	1304	72	462	35	941	67	677	42	9.961E+0E	6.4E+06
1.100	1077	63	790	45	1007	58	1141	64	476	36	844	61	772	45	1.012E+0E	6.5E+06
1.150	1007	59	821	47	1093	62	625	39	571	41	961	66	893	53	9.957E+0E	6.4E+06
1.200	998	59	941	53	778	47	544	35	692	46	1045	71	1047	61	1.046E+0E	6.7E+06
1.250	1094	64	814	47	474	32	660	40	696	47	1138	76	1267	76	1.081E+0E	6.9E+06
1.300	1024	61	511	32	500	33	722	44	766	51	1272	83	1334	78	1.148E+0E	7.3E+06
1.350	794	49	422	27	597	37	739	45	841	55	1376	89	1438	84	1.221E+0E	7.7E+06
1.400	626	40	476	30	657	41	782	48	898	59	1492	96	1656	91	1.312E+0E	8.3E+06
1.450	656	39	562	32	677	40	867	50	1015	62	1704	102	1836	91	1.494E+0E	8.6E+06
1.500	742	41	580	32	704	39	951	51	1083	63	1795	102	1738	90	1.548E+0E	8.6E+06
1.538	745	41	576	31	734	41	1002	54	1115	64	1766	100	1762	91	1.594E+0E	8.9E+06
1.573	724	40	586	32	780	43	1059	57	1196	68	1796	102	1608	84	1.594E+0E	8.9E+06
1.608	703	40	610	34	836	46	1109	60	1301	74	1963	111	1218	65	1.622E+0E	9.1E+06
1.646	696	39	639	35	875	48	1141	61	1378	77	2223	122	743	42	1.648E+0E	9.3E+06
1.684	708	40	674	37	902	50	1183	64	1435	81	2384	130	416	27	1.668E+0E	9.3E+06
1.724	714	40	697	38	917	51	1243	67	1445	82	2145	118	294	21	1.599E+0E	9.0E+06
1.765	703	40	704	39	940	52	1315	72	1449	83	1524	88	293	20	1.445E+0E	8.3E+06
1.808	669	38	702	39	979	55	1369	75	1562	89	843	55	315	20	1.309E+0E	7.7E+06
1.852	621	36	704	39	1029	58	1390	77	1820	102	400	35	313	20	1.277E+0E	7.6E+06
1.896	571	33	712	40	1059	59	1376	76	1983	110	254	28	285	19	1.284E+0E	7.6E+06
1.945	543	32	730	41	1074	60	1372	76	1766	99	268	26	261	18	1.216E+0E	7.2E+06
1.995	524	28	738	38	1064	55	1399	71	1175	62	300	25	257	17	1.037E+0E	5.7E+06
2.046	498	27	724	37	1042	54	1474	75	568	35	304	25	280	18	9.59E+0E	4.9E+06
2.100	463	26	696	36	1036	54	1597	81	210	21	301	24	335	20	7.720E+0E	4.7E+06
2.155	430	24	677	36	1071	56	1681	86	109	17	321	26	429	25	7.817E+0E	4.8E+06
2.213	399	23	675	36	1120	59	1523	78	137	16	364	28	558	31	7.969E+0E	4.8E+06
2.273	380	22	708	37	1130	59	1103	58	188	17	440	31	716	39	7.760E+0E	4.6E+06
2.236	381	22	753	40	999	53	629	35	229	18	563	37	875	47	7.387E+0E	4.4E+06
2.401	402	23	746	40	720	39	306	20	273	20	730	46	1028	56	7.245E+0E	4.4E+06
2.469	416	23	619	32	413	23	179	14	335	22	902	52	1204	62	7.484E+0E	4.3E+06
2.540	398	22	425	23	217	15	194	14	419	26	1076	60	1493	76	8.368E+0E	4.8E+06
2.614	351	20	263	15	164	12	272	16	505	30	1307	72	1894	87	9.964E+0E	5.6E+06
2.691	293	17	179	11	200	13	353	20	572	33	1589	86	2117	109	1.150E+0E	6.3E+06
2.772	256	16	173	11	262	16	412	23	651	38	1884	102	1901	59	1.238E+0E	6.8E+06
2.856	252	16	211	13	316	19	456	26	788	45	2057	112	1345	72	1.249E+0E	6.9E+06
2.944	278	17	261	15	358	21	506	28	997	56	1894	104	774	43	1.188E+0E	6.6E+06
3.037	318	18	310	17	407	22	591	31	1214	63	1412	75	378	23	1.080E+0E	5.8E+06
3.134	358	20	356	19	475	26	717	38	1264	66	847	50	184	17	9.431E+0E	5.3E+06
3.235	400	22	411	22	568	30	879	46	1053	56	426	33	222	18	8.163E+0E	4.8E+06
3.342	460	25	489	26	692	37	1029	54	695	39	274	28	571	33	7.784E+0E	4.7E+06
3.454	549	26	602	28	837	39	1078	50	394	24	437	32	1242	58	8.915E+0E	4.7E+06
3.572	654	32	734	34	938	44	962	45	277	20	885	48	2051	96	1.131E+0E	5.8E+06
3.696	770	37	830	39	912	44	732	35	372	24	1514	76	2710	124	1.404E+0E	7.0E+06
3.826	840	41	834	41	763	38	412	26	633	35	2182	109	2710	131	1.629E+0E	8.2E+06
3.964	812	41	725	36	568	29	394	22	971	51	2686	136	2680	124	1.777E+0E	9.1E+06
4.105	670	34	545	28	498	22	409	22	1288	66	2812	163	2345	117	1.952E+0E	1.0E+07
4.262	498	26	398	21	361	20	556	29	1561	80	2706	138	2522	126	1.952E+0E	1.0E+07
4.424	387	22	350	19	449	24	809	41	1732	88	2598	133	2586	130	2.004E+0E	1.0E+07
4.585	415	23	434	23	660	34	1123	57	1712	87	2479	126	2018	121	1.777E+0E	9.0E+06
4.776	615	32	648	33	952	48	1405	70	1930	77	2062	104	1063	53	1.777E+0E	9.0E+06
4.965	563	28	942	47	1225	61	1518	75	1279	64	1290	66	328	18	1.439E+0E	7.3E+06
5.173	1370	68	1211	60	1342	67	1398	69	941	48	520	29	73	7		

TABLE 3
DEUTERON ENERGY 2.3 MeV

DEUTERON ENERGY ANGLE NEUTRON ENERGY	2.30		30		45		60		90		120		150		INTEGRATED 0-180	
	COUNT	ERROR	COUNT	ERROR	COUNT	ERROR	COUNT	ERROR	COUNT	ERROR	COUNT	ERROR	COUNT	ERROR	COUNT	ERROR
0.100	41665	10653	36248	9190	34343	8281	33690	7989	33763	7951	31522	7501	34661	8193	4.245E+05	1.0E+09
0.150	46535	2784	15010	2551	13571	2307	12036	2082	11277	1983	10558	1856	11377	2012	1.494E+09	2.6E+08
0.200	11740	1073	10544	1016	9076	858	8253	798	7418	747	7401	731	8127	807	1.030E+05	1.0E+08
0.250	10841	699	9599	638	8013	543	7066	495	6147	455	6491	462	7081	507	8.887E+08	6.5E+07
0.300	10514	610	9408	557	7460	453	6539	409	5524	364	5902	375	6285	404	8.164E+08	5.1E+07
0.350	10340	570	8725	493	6741	390	5826	346	5002	310	5178	314	5590	341	7.345E+08	4.4E+07
0.400	9732	526	8002	443	6040	342	4837	284	4378	264	4763	279	5194	305	6.561E+08	3.8E+07
0.450	9438	496	7472	402	4906	275	4463	253	3980	231	4324	245	4703	268	5.942E+08	3.4E+07
0.500	5691	485	6551	341	4675	250	4198	227	3851	213	4107	222	4618	250	5.604E+08	3.0E+07
0.550	9048	456	6278	326	4610	245	4149	223	3821	209	4128	221	4562	245	5.566E+08	3.0E+07
0.600	8738	445	6160	322	4475	239	3892	211	3565	197	4123	221	4574	245	5.393E+08	2.9E+07
0.650	8961	455	6162	320	4252	226	3721	201	3617	197	4077	217	4240	226	5.277E+08	2.6E+07
0.700	5831	499	6443	335	4421	234	3853	207	3878	209	4038	215	3164	175	5.252E+08	2.8E+07
0.750	10614	557	6675	358	4434	244	3946	218	3909	217	3914	215	2518	148	5.171E+08	2.9E+07
0.800	11075	587	6754	365	4399	242	3798	211	3848	215	2893	165	2439	143	4.831E+08	2.7E+07
0.850	11340	593	6520	348	4172	227	3642	200	3840	210	2135	124	2325	134	4.513E+08	2.5E+07
0.900	11964	624	6688	356	4134	224	3689	201	3771	206	2169	124	2443	138	4.559E+08	2.5E+07
0.950	12330	639	6533	345	3922	212	3574	194	3546	192	2037	116	1851	107	4.282E+08	2.3E+07
1.000	12625	661	6440	343	3874	211	3505	192	2358	134	2067	117	923	63	3.707E+08	2.1E+07
1.050	13002	685	6271	337	3744	205	3384	186	1887	111	2006	113	913	60	3.448E+08	2.0E+07
1.100	13708	730	6567	356	3777	208	3399	188	2023	117	1221	75	566	62	3.371E+08	1.9E+07
1.150	14207	765	6564	359	3730	208	3258	182	2086	121	831	56	569	63	3.276E+08	1.9E+07
1.200	15316	833	6579	364	3791	212	2492	143	2398	137	945	60	1083	68	3.255E+08	1.8E+07
1.250	16345	896	6852	381	3422	193	2115	124	2167	125	975	61	1173	73	3.151E+08	1.8E+07
1.300	15631	870	7111	399	2532	148	2066	122	1332	83	1000	63	1272	75	2.803E+08	1.7E+07
1.350	16975	953	6275	356	2041	123	2091	124	943	63	1069	67	1376	85	2.602E+08	1.6E+07
1.400	20168	1140	4133	241	1938	117	2292	136	938	62	1137	71	1454	89	2.502E+08	1.5E+07
1.450	13800	756	2008	120	2077	118	2664	148	1108	67	1229	72	1620	88	2.160E+09	1.2E+07
1.500	4167	223	1690	97	2319	123	2524	132	1233	69	1292	72	1620	88	2.046E+08	1.1E+07
1.538	1023	83	1858	103	2493	131	2068	110	1275	71	1319	73	1505	83	1.984E+08	1.1E+07
1.572	568	63	2124	115	2598	137	1591	88	1310	73	1375	76	1505	83	1.948E+08	1.1E+07
1.608	1293	78	2370	128	2480	132	1268	73	1335	75	1449	80	1408	79	1.908E+08	1.1E+07
1.644	1783	100	2478	132	2102	113	1170	68	1351	76	1500	82	1332	75	1.916E+08	1.1E+07
1.684	2026	111	2394	129	1663	92	1261	72	1397	78	1512	84	1479	83	1.912E+08	1.1E+07
1.724	1996	109	2091	115	1337	77	1421	80	1465	82	1512	84	1593	89	1.911E+08	1.1E+07
1.765	1788	99	1685	95	1214	71	1546	87	1545	87	1467	82	1593	89	1.911E+08	1.1E+07
1.808	1452	82	1343	78	1262	73	1592	89	1617	91	1432	81	1569	88	1.892E+08	1.1E+07
1.852	1088	64	1181	70	1380	79	1588	90	1694	96	1466	83	1339	76	1.871E+08	1.1E+07
1.898	818	51	1173	69	1468	83	1561	88	1754	99	1568	88	980	58	1.851E+08	1.1E+07
1.945	716	45	1241	73	1518	86	1563	89	1798	102	1662	93	651	42	1.843E+08	1.1E+07
1.995	721	42	1280	68	1518	79	1591	83	1806	93	1574	81	432	30	1.791E+08	9.5E+06
2.046	723	41	1257	67	1484	78	1626	85	1808	94	1265	66	345	26	1.791E+08	9.5E+06
2.100	669	38	1207	65	1443	76	1656	87	1862	97	866	48	366	27	1.594E+08	8.6E+06
2.155	582	35	1170	64	1419	75	1678	88	1981	104	544	34	457	30	1.555E+08	8.5E+06
2.213	501	31	1134	63	1367	76	1663	89	2038	107	368	26	574	35	1.534E+08	8.5E+06
2.273	465	29	1109	62	1394	75	1644	88	1901	100	339	25	696	41	1.496E+08	8.3E+06
2.336	473	30	1097	61	1409	77	1652	89	1520	82	416	28	816	47	1.418E+08	7.9E+06
2.401	514	32	1108	63	1442	79	1715	93	1047	59	548	34	948	54	1.345E+08	7.6E+06
2.469	562	32	1129	61	1478	77	1791	92	661	39	688	38	1689	59	1.309E+08	7.1E+06
2.540	595	34	1181	63	1546	81	1812	93	473	31	830	45	1268	67	1.340E+08	7.3E+06
2.614	606	35	1287	69	1640	86	1689	88	471	30	974	53	1515	80	1.421E+08	7.8E+06
2.691	606	35	1406	75	1652	87	1652	87	571	34	1090	59	1777	94	1.478E+08	8.0E+06
2.772	645	37	1485	80	1519	81	989	55	705	40	1187	64	1991	106	1.499E+08	8.2E+06
2.856	733	42	1439	78	1245	68	823	43	832	47	1282	70	2029	105	1.481E+08	8.2E+06
2.944	818	46	1249	69	947	53	652	39	935	52	1383	76	1804	98	1.432E+08	8.0E+06
3.037	821	44	1007	54	746	42	755	42	1026	54	1453	75	1401	74	1.381E+08	7.4E+06
3.134	711	39	803	45	679	39	943	51	1104	59	1408	74	983	54	1.325E+08	7.2E+06
3.235	575	33	706	40	734	41	1112	59	1180	63	1239	66	742	44	1.288E+08	7.1E+06
3.342	513	30	720	41	856	47	1192	64	1242	66	1030	56	781	46	1.289E+08	7.1E+06
3.454	552	29	812	41	992	48	1190	57	1265	60	905	45	1078	54	1.342E+08	6.6E+06
3.572	634	33	942	47	1110	54	1165	56	1232	60	926	47	1525	74	1.444E+08	7.1E+06
3.656	709	36	1096	54	1219	60	1183	58	1164	57	1087	54	2006	57	1.590E+08	7.9E+06
3.826	779	40	1291	65	1351	67	1250	62	1112	57	1390	68	2486	122	1.708E+08	9.0E+06
3.964	878	46	1506	77	1470	75	1288	66	1108	58	1672	85	2952	148	2.011E+08	1.0E+07
4.109	999	52	1643	84	1478	75	1212	62	1168	61	2026	103	3272	164	2.191E+08	1.1E+07
4.262	1106	57	1663	85	1378	71	1087	57	1355	70	2425	122	3352	169	2.344E+08	1.2E+07
4.424	1126	59	1553	80	1229	64	1028	54	1681	86	2728	138	3071	155	2.442E+08	1.3E+07
4.565	1049	55	1381	72	1136	59	1129	59	2067	105	2724	137	2436	123	2.440E+08	1.2E+07
4.776	920	50	1287	67	1201	62	1397	71	2339	117	2377	119	1623	62	2.337E+08	1.2E+07
4.969	967	50	1396	71	1460	74	1748	88	2335	116	1841	92	874	45	2.165E+08	1.1E+07
5.173	1201	61	1754	89	1861	93	2035	102	2040	102	1244	63	344	20	1.957E+08	9.9E+06
5.390	1621	82	2262	113	2226	111	2086	104	1540	77	674	35	86	7	1.408E+08	7.2E+06
5.621	2036	101	2677	133	2315	116	1841	92	975	49	268	16	28	0	0	0
5.867	2189	108	2721	134	2078	102	1388	69	481	25	84	8	0	0	0	0
6.130	1943	95	2287	112	1533	75	868	43	159	10	56	6	0	0	0	0
6.411	1436	71	1562	79	932	47	424	22	23	5	0	0	0	0	0	0
6.711	848	44	865	45	433	23	134	9	5	0	0	0	0	0	0	0
7.074	347	20	316	19	120	9	16	5	0	0	0	0	0	0	0	0
7.380	64	6	41	6	8	4	0	0								

TABLE 4

DEUTERON ENERGY 2.8 MeV

DEUTERON ENERGY ANGLE	2.80		30		45		60		90		120		150		INTEGRATED 0-180	
DEUTERON ENERGY	COUNT	ERROR	COUNT	ERROR	COUNT	ERROR	COUNT	ERROR	COUNT	ERROR	COUNT	ERROR	COUNT	ERROR	COUNT	ERROR
C.10C	82956	17863	59777	14804	57069	14274	53345	12119	50656	11217	47604	10175	47916	10964	6.530E+09	1.5E+09
0.150	29400	4719	24434	4061	22885	3854	20659	3355	18565	3022	16886	2746	17492	2944	2.449E+09	4.0E+08
C.25C	17951	1511	15615	1438	14131	1313	13007	1122	11827	1031	11466	991	12420	1135	1.594E+09	1.4E+08
0.250	15924	521	13530	872	12238	811	11247	684	10099	624	10106	614	10382	666	1.373E+09	3.6E+07
C.35C	14768	801	12492	749	11154	668	10318	575	9096	515	8663	488	9214	553	1.238E+09	7.1E+07
0.300	12378	724	11719	652	10289	586	9407	507	8223	444	7443	407	7812	452	1.104E+09	6.1E+07
C.45C	11616	610	10368	579	8932	502	8160	447	7131	385	6431	350	6616	379	9.634E+08	5.3E+07
0.400	12475	610	10378	536	8371	456	7653	400	5978	315	5509	295	5967	332	8.563E+08	4.6E+07
C.55C	12775	610	9987	517	8283	429	7559	378	5536	284	5088	261	5640	300	8.255E+08	4.2E+07
0.500	12936	626	10179	516	8433	429	7380	369	5171	266	4906	252	5472	290	8.034E+08	4.1E+07
C.65C	13186	641	10133	517	7943	414	6084	312	4647	243	4903	253	5451	289	7.531E+08	3.9E+07
0.600	14494	722	10764	548	6936	367	5657	290	4394	229	4734	244	5271	278	7.203E+08	3.7E+07
C.75C	15393	796	10435	552	7092	384	5750	295	4690	242	4741	245	5221	277	7.357E+08	3.8E+07
0.600	15703	821	9929	532	6722	368	5274	285	4758	256	4869	260	5273	288	7.466E+08	4.0E+07
C.85C	15904	841	9556	527	6662	356	4763	255	4616	247	4567	243	4933	268	6.940E+08	3.7E+07
0.500	16638	839	9737	514	5962	322	4761	254	4629	247	4578	243	4794	260	6.820E+08	3.6E+07
C.95C	16295	848	9743	509	4891	266	4588	242	4464	237	4403	233	4212	228	6.445E+08	3.4E+07
1.00C	16992	883	7963	425	4737	269	4441	238	4368	234	4292	227	3150	179	5.960E+08	3.0E+07
1.050	16234	850	7023	379	4578	252	4388	236	4419	238	4167	223	3298	183	5.823E+08	3.2E+07
1.100	14681	779	7128	338	4590	255	4467	243	4541	240	3566	195	3215	181	5.673E+08	3.1E+07
1.150	15308	823	7182	395	4599	258	4415	243	4621	253	2842	159	3592	201	5.576E+08	3.1E+07
1.200	16324	886	7416	410	4675	263	4469	248	4721	261	2825	158	3015	171	5.566E+08	3.1E+07
1.250	16532	905	7414	414	4613	262	4481	250	4774	265	2865	152	1996	99	5.352E+08	3.0E+07
1.300	17292	961	7621	431	4560	262	4528	256	4453	251	3142	170	1586	86	5.347E+08	3.0E+07
1.350	18129	1010	7653	436	4496	261	4589	262	3622	208	2940	164	1742	100	5.075E+08	2.9E+07
1.400	19186	1086	7543	434	4495	263	4711	271	3031	180	2093	123	1699	104	4.691E+08	2.7E+07
1.450	20015	1072	7717	420	4572	253	4840	263	3046	160	1366	80	1649	96	4.538E+08	2.5E+07
1.500	20371	1027	7821	401	4533	238	5029	258	3249	169	1438	73	1642	91	4.736E+08	2.5E+07
1.550	20714	1044	7771	399	4567	239	5074	259	3463	179	1544	93	1642	90	4.839E+08	2.5E+07
1.575	21473	1091	7778	402	4728	248	4902	253	3586	186	1595	86	1561	86	4.652E+08	2.5E+07
1.600	22403	1148	7722	433	4880	257	4409	230	3296	173	1610	87	1486	84	4.652E+08	2.5E+07
1.644	23069	1182	7568	395	4828	254	3789	199	2596	137	1618	87	1647	83	4.257E+08	2.3E+07
1.684	23464	1210	7672	403	4566	243	3369	179	1924	105	1627	88	1415	80	3.748E+08	2.1E+07
1.724	22805	1190	8012	423	4061	219	3220	173	1551	87	1607	83	1464	83	3.703E+08	2.0E+07
1.765	22678	1163	8072	425	3403	191	3136	180	1515	85	1584	87	1534	87	3.767E+08	2.0E+07
1.808	23641	1256	7179	386	3072	171	3640	197	1656	93	1590	89	1598	91	3.722E+08	2.0E+07
1.852	27761	1486	5428	257	2957	166	3891	212	1803	101	1599	39	1619	53	3.717E+08	2.1E+07
1.898	27885	1492	3591	200	3073	171	3698	201	1874	104	1579	88	1581	51	3.502E+08	1.9E+07
1.945	19458	1052	2511	145	3342	180	3062	169	1922	107	1569	88	1614	93	3.114E+08	1.7E+07
1.995	8066	400	2359	125	3487	176	2296	117	1965	100	1553	80	1774	92	2.741E+08	1.4E+07
2.044	1326	90	2768	143	3219	164	1758	92	1991	102	1523	73	1935	100	2.523E+08	1.3E+07
2.100	353	54	3115	160	2573	134	1574	83	1961	101	1514	79	1851	94	2.395E+08	1.3E+07
2.155	1600	96	2955	154	1918	104	1645	87	1904	99	1576	93	1468	74	2.275E+08	1.2E+07
2.213	2490	130	2273	121	1505	84	1771	94	1862	98	1703	89	999	57	2.133E+08	1.1E+07
2.273	2186	115	1554	86	1384	78	1846	98	1857	98	1773	93	740	46	2.022E+08	1.1E+07
2.336	1350	74	1127	66	1432	80	1847	98	1850	98	1618	86	765	47	1.922E+08	1.1E+07
2.401	603	42	1065	63	1535	86	1825	98	1888	102	1288	70	545	56	1.865E+08	1.0E+07
2.465	480	32	1196	66	1602	85	1799	92	2012	103	984	53	1207	60	1.876E+08	9.9E+06
2.540	591	35	1324	72	1617	86	1778	92	2185	112	864	47	1434	76	1.953E+08	1.0E+07
2.614	739	42	1385	75	1609	87	1760	92	2195	113	928	50	1612	65	2.012E+08	1.1E+07
2.651	785	44	1380	75	1580	86	1737	91	1852	97	1065	57	1702	51	1.948E+08	1.0E+07
2.772	798	45	1382	76	1576	86	1793	95	1365	73	1214	65	1780	96	1.858E+08	1.0E+07
2.856	833	47	1415	79	1633	90	1930	104	1005	56	1318	71	1843	100	1.823E+08	1.0E+07
2.944	877	50	1407	83	1787	99	2062	111	894	51	1348	73	1837	100	1.850E+08	1.0E+07
3.037	552	51	1670	88	2039	106	2051	105	980	52	1339	69	1805	94	1.917E+08	1.0E+07
3.134	1125	60	2019	106	2236	116	1795	93	1100	58	1313	69	1746	92	1.947E+08	1.0E+07
3.235	1425	77	2418	126	2182	114	1438	76	1153	61	1307	69	1647	88	1.943E+08	1.0E+07
3.342	1845	97	2518	132	1839	98	1180	63	1135	61	1366	72	1588	85	1.832E+08	9.8E+06
3.454	1990	92	2140	100	1426	69	1089	52	1130	54	1503	70	1686	80	1.781E+08	8.5E+06
3.572	1078	79	1562	76	1157	58	1111	54	1235	59	1652	78	1891	91	1.799E+08	8.7E+06
3.656	1143	56	1168	60	1092	56	1181	58	1479	71	1718	82	2038	99	1.878E+08	9.2E+06
3.826	791	42	1098	58	1188	62	1302	65	1781	87	1695	83	2158	117	2.014E+08	1.0E+07
3.964	793	43	1246	66	1378	72	1501	76	1958	98	1684	85	2529	124	2.219E+08	1.1E+07
4.105	990	52	1450	76	1601	83	1732	88	1896	96	1830	93	3317	167	2.488E+08	1.3E+07
4.262	1172	61	1695	88	1846	95	1923	97	1771	90	2251	114	4178	210	2.825E+08	1.4E+07
4.424	1260	65	1965	131	2041	105	1968	100	1760	90	2827	143	4212	213	3.053E+08	1.6E+07
4.595	1311	68	2196	112	2100	107	1876	95	1932	98	3211	162	3286	166	3.060E+08	1.6E+07
4.776	1403	72	2337	118	2035	104	1797	91	2270	114	3161	158	2303	116	2.968E+08	1.5E+07
4.965	1565	79	2373	119	1952	99	1843	92	2630	131	2755	137	1623	82	2.853E+08	1.4E+07
5.173	1759	88	2339	118	1947	101	2032	102	2789	139	2200	109	999	51	2.680E+08	1.3E+07
5.390	1926	97	2345	118	2277	111	2288	114	2604	130	1515	76	409	23	2.403E+08	1.2E+07
5.621	2070	103	2568	129	2567	128	2470	123	2116	105	781	39	89	9	2.385E+08	1.1E+07
5.867	2268	112	3039	150	2871	142	2405	118	1440	71	235	13	15	6	1.778E+08	9.0E+06
6.130	2466	119	3423	167	2820	138	1998	97	744	37	25	6	0	0	1.440E+08	7.2E+06
6.411	2563	117	3294	163	2317	115	1388	69	244	14	4	0	0	0	1.005E+08	5.5E+06
6.711	1878	97	2515	130	1545	80	763	40	26	4	0	0	0	0	6.693E+07	3.7E+06

TABLE 5
CALCULATED MAXIMUM NEUTRON ENERGIES (MeV)
EXPECTED FROM THE ${}^9\text{Be}(d,n){}^{10}\text{B}$ REACTION

Deuteron Energy (MeV)	Angle (degrees)	0	30	45	60	90	120	150
1.4		5.71	5.60	5.49	5.33	4.98	4.65	4.42
1.8		6.13	6.01	5.86	5.68	5.27	4.89	4.62
2.3		6.64	6.50	6.33	6.12	5.63	5.19	4.88
2.8		7.15	6.99	6.79	6.55	6.00	5.49	5.15

TABLE 6

ANGULAR DISTRIBUTIONS FROM THE THICK TARGET ${}^9\text{Be}(d,n){}^{10}\text{B}$

REACTION FOR NEUTRONS WITH ENERGIES ABOVE THREE

NEUTRON ENERGY THRESHOLDS

Angle (degrees)		0	30	45	60	90	120	150
Deuteron Energy (MeV)	Neutron Threshold Energy (MeV)	neutrons $\text{cm}^{-2} \mu\text{C}^{-1}$ at 100 cm						
1.4	0.075	5924	5657	5257	4785	4256	4742	4864
	0.25	4571	4366	4085	3705	3249	3622	3728
	0.95	2283	2829	2937	2790	2622	3137	3269
1.8	0.075	13086	7823	7508	8102	7628	10598	9111
	0.25	10933	6377	6053	6544	6125	8456	7186
	0.95	4501	3751	4104	4621	4394	6281	5585
2.3	0.075	25365	20028	15981	14373	12886	12301	12483
	0.25	21748	16822	13081	11654	10275	9553	9769
	0.95	14524	11778	9519	8537	7362	6722	6886
2.8	0.075	45946	31650	25227	22580	19420	17183	17528
	0.25	39385	26530	20422	18161	15333	13357	13595
	0.95	29396	19063	14753	13296	11280	9408	9355

TABLE 7

TOTAL NEUTRON YIELD ABOVE DIFFERENT THRESHOLD ENERGIES

Deuteron Energy (MeV)	1.4	1.8	2.3	2.8
Threshold Energy (MeV)	Yield (neutrons μC^{-1}) $\div 10^8$			
0.075	6.016	10.92	17.60	26.68
0.25	4.592	8.761	14.20	21.33
0.95	3.647	6.220	10.12	15.37
0 (extrapolated values)	7.2	12.3	20.0	30.0

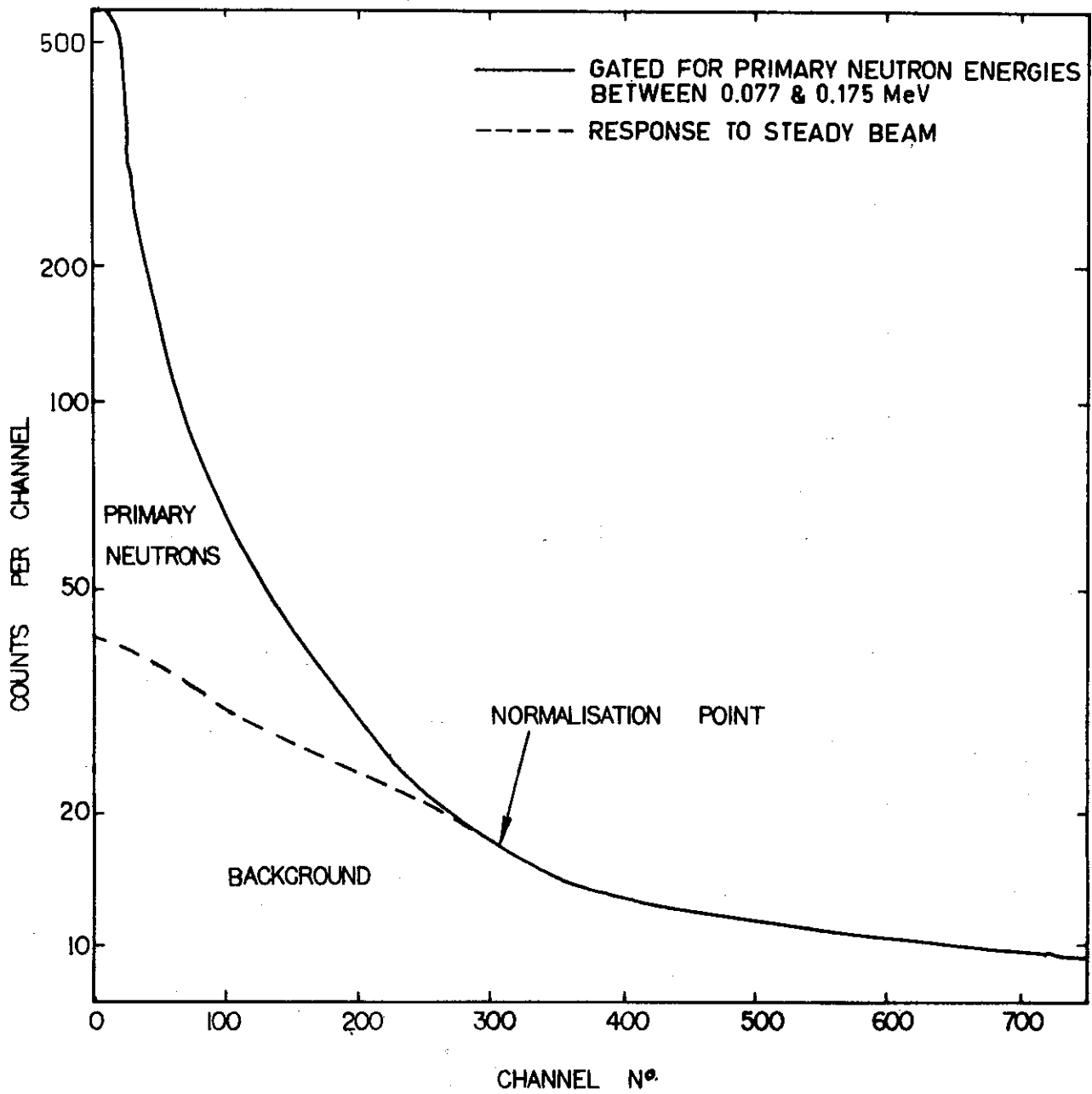


FIGURE 1. PULSE HEIGHT SPECTRA FROM SCINTILLATOR

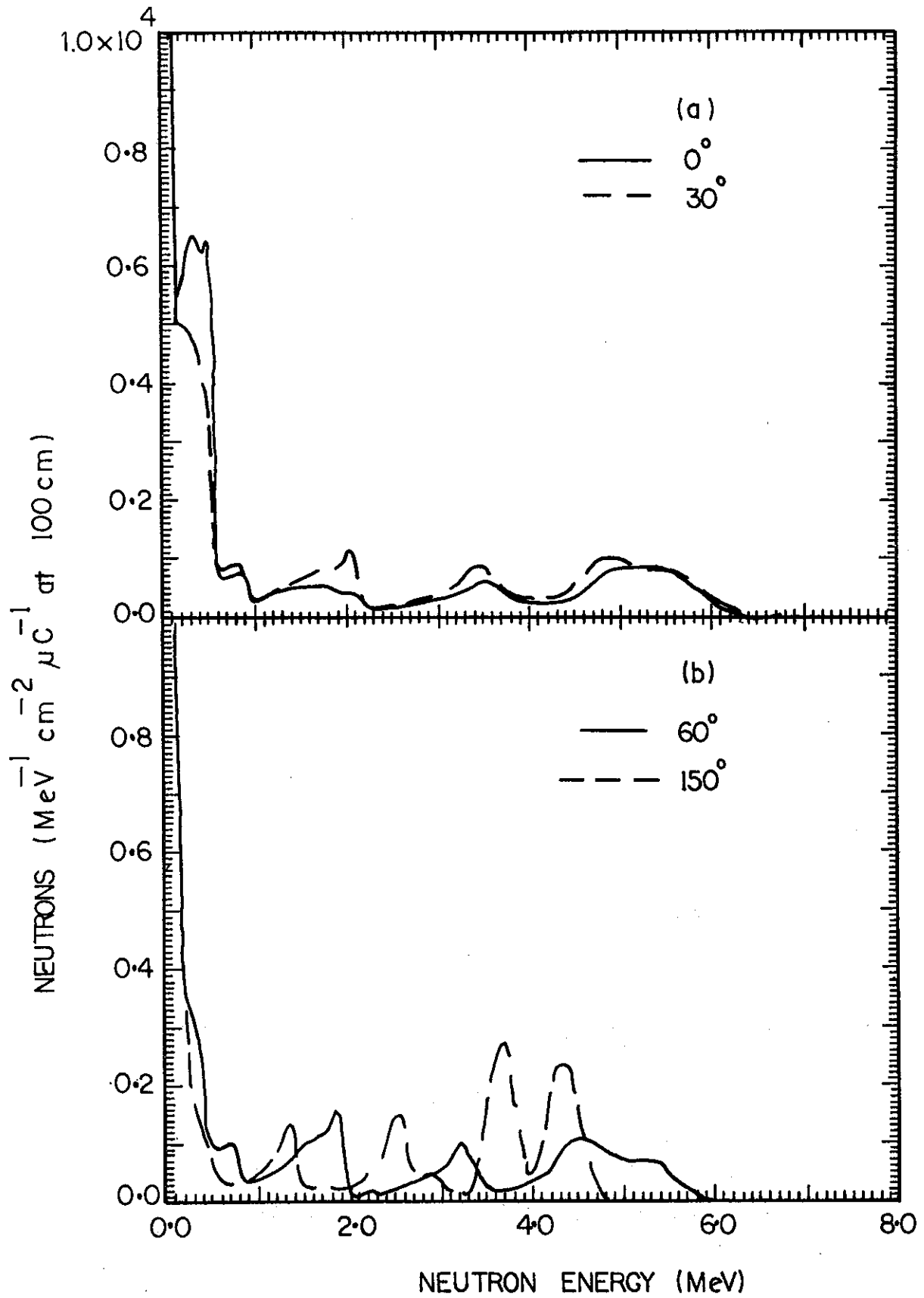


FIGURE 2. ANGLE-DEPENDENT NEUTRON ENERGY SPECTRA FROM THE ${}^9\text{Be}(d,n){}^{10}\text{B}$ REACTION FOR DEUTERON ENERGY 1.4 MeV

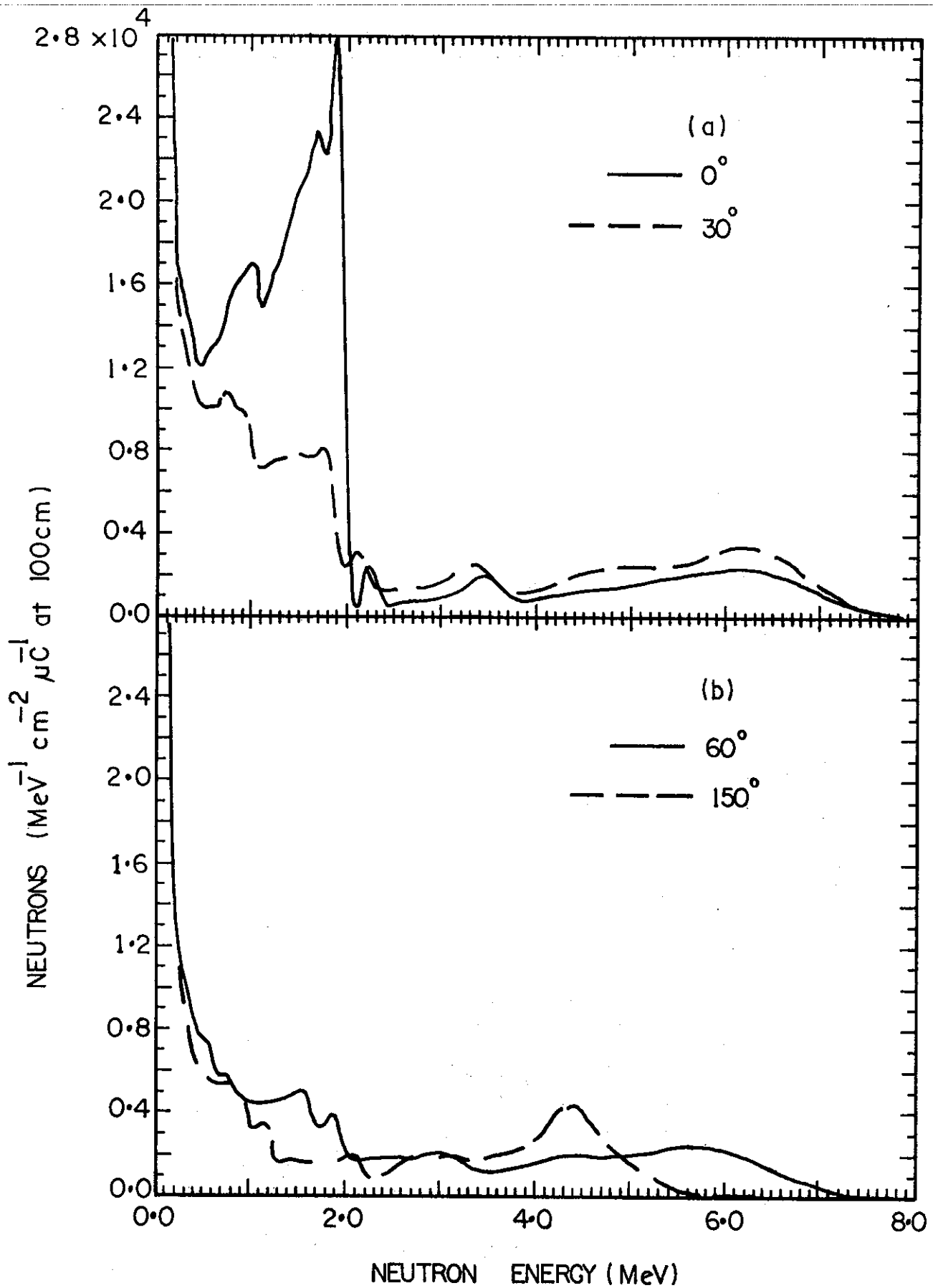


FIGURE 3. ANGLE-DEPENDENT NEUTRON ENERGY SPECTRA FROM THE ${}^9\text{Be}(d,n){}^{10}\text{B}$ REACTION FOR DEUTERON ENERGY 2.8 MeV

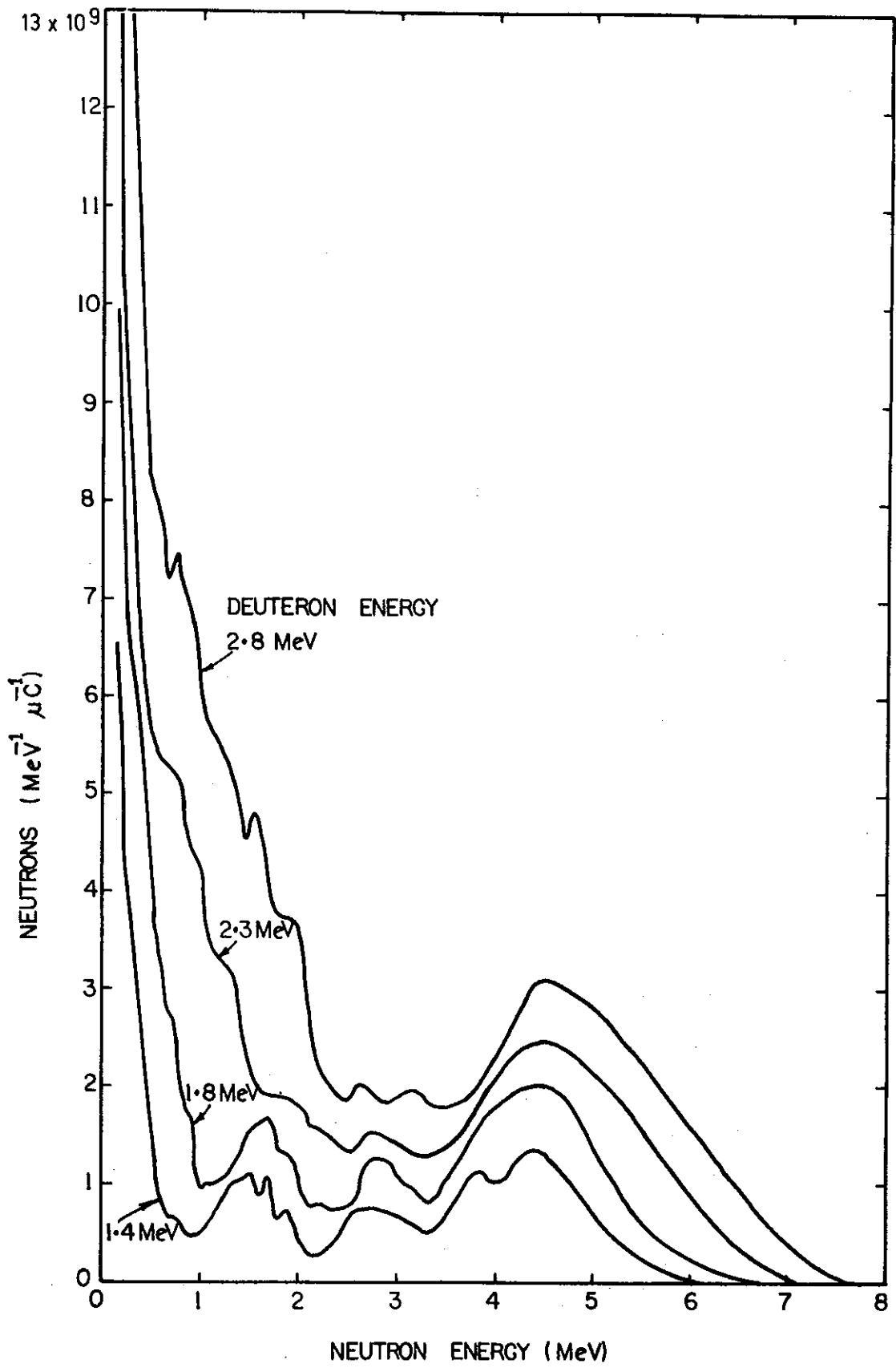


FIGURE 4. ANGLE-INTEGRATED NEUTRON ENERGY SPECTRA

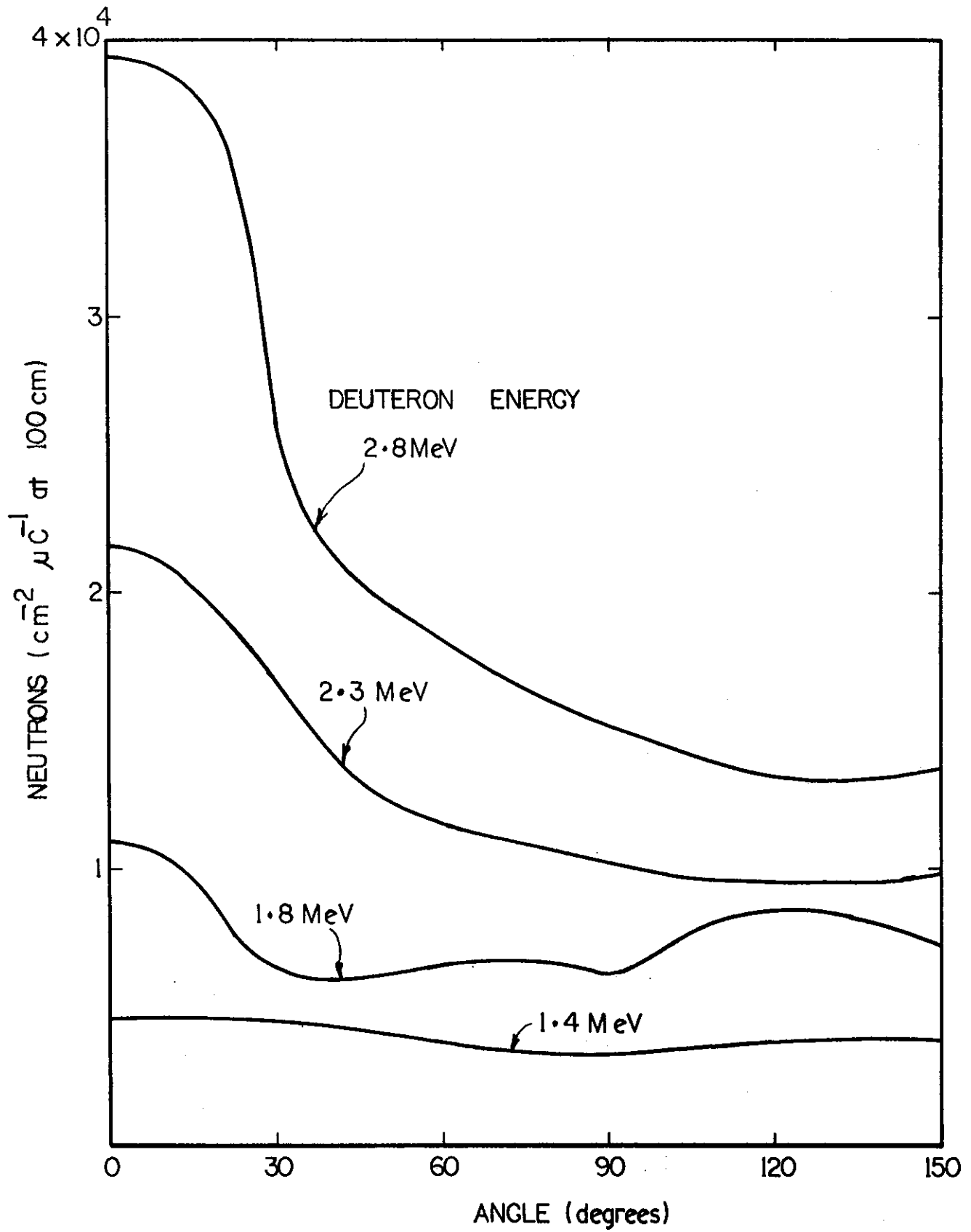


FIGURE 5. ANGULAR DISTRIBUTIONS FROM THE THICK TARGET ${}^9\text{Be}(d,n){}^{10}\text{B}$ REACTION FOR NEUTRONS WITH ENERGIES GREATER THAN 0.25 MeV

